Progress in Physics (23)

Graphene on Close-Packed Metal Surfaces – Long-range Order and Band Gap Engineering

F. D. Natterer, S. Rusponi, and H. Brune
Institute of Condensed Matter Physics, Ecole Polytechnique Fédérale de Lausanne, Station 3, CH-1015 Lausanne

Graphene (g) is a 2D honeycomb lattice made of carbon atoms with the conduction electrons in sp^2 hybridized Bloch states. Its exceptional charge carrier mobility and optical transparence of 98 % make graphene an ideal material for fast transistors [1] and for solar cell top electrodes, respectively. Close to the K points of the Brillouin zone, the bands have a linear dispersion that is well described by the relativistic Dirac equation for massless neutrinos. The resulting Dirac cones of the conduction and valence bands touch each other at their summits at the Dirac point located at the Fermi level E_F. Therefore freestanding graphene is a zero-gap semiconductor. However, most electronic device applications require a band gap.

Theory has suggested that a gap may derive from an external long-range periodic potential [2-4]. Such a potential is created when putting graphene onto a lattice mismatched close-packed metal surface. The resulting moiré structures exhibit periodic stacking alternations between C rings localized on-top of metal atoms, implying that both C atoms of the g unit cell are on substrate hollow sites, and C rings centered above one or the other of the two non-equivalent substrate hollow sites, implying that either one of the two C atoms is localized on-top of a substrate atom. The binding of graphene to the substrate has a significant van der Waals contribution, however, directed chemical bonds can be formed where C atoms are on-top of substrate atoms. Their strength depends on the substrate, it increases going from Ir via Pt, Rh to Ru. For g/Ir(111) it has been shown that adsorbing metal clusters on-top gives rise to very strong such bonds as it leads to a local sp^3 hybridization between the first C atom and its underlying substrate atom and the other with a cluster atom on top [5]. This is expected to strongly enhance the corrugation of the electron potential. We show the experimental realization of this concept of band gap engineering for equidistant Ir clusters grown on g/Ir(111). From angle-resolved photo-electron spectroscopy (ARPES) and low-temperature scanning tunneling spectroscopy experiments we find that long range order in graphene is mandatory for its electronic structure to evolve. Therefore we discuss first the preparation methods yielding ideal long-range order for the case of g/Ru(0001) until we turn to g/Ir(111) and end with perspectives.

Graphene may be prepared by numerous methods. Among these is the exfoliation from highly oriented pyrolytic graphite with scotch tape and transfer to a substrate [6]. For the growth of graphene on well defined atomically clean single crystal surfaces and in ultra high vacuum one exposes the surface to a partial pressure of a C-containing molecule, either at low temperature with subsequent annealing [2, 7-9], or directly at high temperature where the molecules immediately dissociate by the catalytic activity of the substrate, leaving C at the surface while the rest of the molecule desorbs, and the growth therefore corresponds to chemical vapor deposition (CVD). Surface segregation of bulk dissolved carbon impurities [10-12] or molecular beam epitaxy (MBE) from high purity carbon rods at elevated temperatures [13] are further alternatives. We discuss four of these growth techniques for the case of a Ru(0001) substrate and focus on the resulting long-range order.

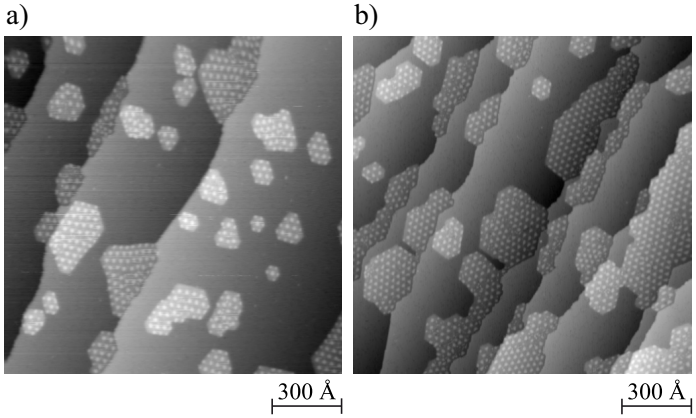

FIG. 1. Graphene growth by chemisorption and dissociation cycles of ethylene on Ru(0001). a) STM constant current image after first cycle, leading to a g coverage of Θ = 0.23 ML.
b) STM image after second step showing Θ = 0.43 ML (one cycle consists of exposure to 5 L (1 Langmuir = 1.33 x 10^{-6} mbar s) C_2H_4 at T_{ads} = 300 K, dissociation and H_2 desorption at T_{diss} = 1100 K, STM parameters V_t = -1.0 V, I_t = 316 pA, T = 300 K).

Chemisorption of a saturated monolayer (ML) of ethylene (C_2H_4) at room temperature, followed by thermal dehydrogenation at T_{diss} = 1100 K, gives rise to graphene islands visible on the atomic substrate terraces in Fig. 1a). The periodic superstructure is due to the (23x23) moiré pattern [14-16]. On Pt(111), chemisorbed ethylene has at 300 K a saturation coverage leading after decomposition to 0.25 ML g [8]. On Ru(0001) we measure after one chemisorption and annealing cycle a graphene coverage of Θ = (0.23 ± 0.05) ML in agreement with this value. A second cycle yields a cover age of Θ = (0.43 ± 0.05) ML and triggers coalescence of graphene islands, as seen in Fig. 1b). Since there are many translational domains of the moiré structure, island coalescence leads with a high probability to domain walls. A third cycle leads to Θ = (0.54 ± 0.05) ML and therefore the coverage as a function of the number of cycles n is described by $\Theta = 1 - (1 - 0.24)^n$. This is the expected law for ethylene only chemisorbing on the bare metal surface. The growth by sequential chemisorption and decomposition has the advantage of being self-limiting, one asymptotically

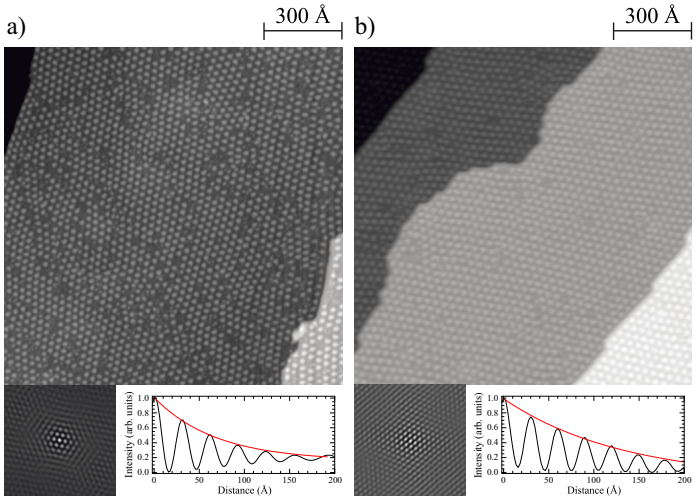

FIG. 2. Temperature-dependent long-range order of graphene grown by ethylene CVD at a) T_{CVD} = 1100 K (20 L) and b) at T_{CVD} = 1670 K (80 L). After exposure the temperature is held for 2 min and then lowered to room temperature with $\dot{T}$ = -7 K/s. The lower left panels are 2D autocorrelation images and the lower right cuts through them showing exponential decay defining the autocorrelation length (V_t = -1.0 V, I_t = 316 pA).

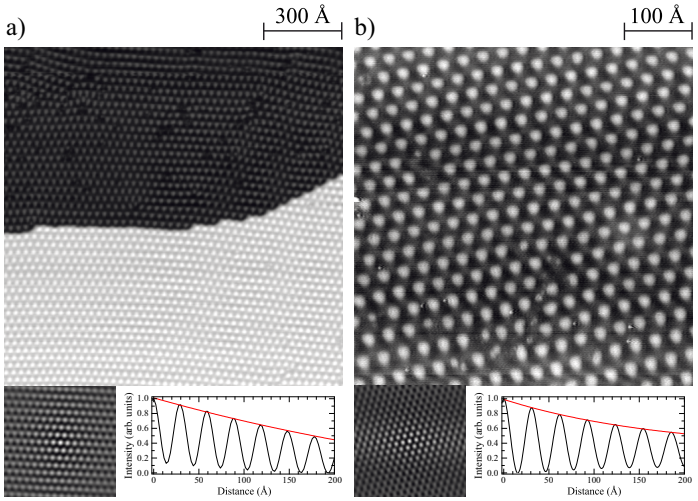

FIG. 3. a) Graphene layer with an autocorrelation length of Λ = 238 ± 12 Å obtained from intentionally dissolving carbon into bulk during CVD and its subsequent controlled surface segregation during slow cooling (127 L C_2H_4 at T_{CVD} = 1540 K, $\dot{T}$ = -0.1 K/s, V_t = -1 V, I_t = 316 pA).
b) Graphene growth during a short flash to T = 1570 K of a freshly prepared Ru surface due to surface segregation of residual bulk dissolved carbon from previous graphene preparation cycles (V_t = -0.88 V, I_t = 150 pA).

approaches a single layer graphene and no second layer will grow, however, it suffers from the many domain walls limiting the long-range order.
In CVD graphene growth the Ru(0001) surface is exposed to ethylene at $T_{CVD} \geqslant$ 1000 K. However, C dissolves into Ru bulk, and in addition, the solubility of interstitial carbon in ruthenium shows a strong temperature dependence, it is six times higher at 1540 K than at 1000 K [10]. In order to prevent diffusion into bulk, as well as surface segregation of already dissolved C, CVD growth has to be taken out at not too high temperature and the sample has to be rapidly quenched afterwards. Both requirements are somewhat in contradiction with best order. For the quench the best compromise is $\dot{T}$ = -7 K/s and the influence of the growth temperature is illustrated in Fig. 2. In both cases there is exactly a full monolayer graphene and it is evident from visual inspection that the higher exposure temperature leads to better long-range order. This is quantified by the exponential decay lengths of the 2D autocorrelation functions [17]. A signicantly higher value of Λ = (131 ± 8) Å is found for T_{CVD} = 1670 K while the autocorrelation decays with Λ = (68 ± 12) Å for T_{CVD} = 1100 K. When disregarding the bulk solubility, also CVD is self-limiting since we find that growth of the second monolayer requires significantly higher exposures. The delicate issue with CVD growth is the bulk solubility at the temperature giving best order. This can be turned into an advantage as shown below, however, it renders control on the graphene coverage more difficult.

The third growth method combines CVD surface growth with deliberate loading of the surface region with carbon which is then segregated by a very slow cool down [12]. With optimizing the parameters we achieved very well ordered graphene layers as seen in Fig. 3a with an autocorrelation length of Λ = (238 ± 12) Å, which is the most prominent argument for this technique. However, one needs to keep track of the coverage as multiple layers may be nucleated if sufficient interstitial carbon has been created before [18]. The fourth growth technique is the mere segregation of Ru bulk dissolved carbon impurities. The amount of C present in commercial Ru crystals suffices to create many times relatively well ordered graphene layers by a flash to T = 2000 K [11]. However, these layers might suffer from the other elements than C that may also segregate. After many sputter, oxygen glowing, and flash cycles, Ru gets entirely clean [11] and then one may load it with only C in the way described above. When a sample is used many times before for CVD some of the C goes deep such that a flash might reveal the preparation history of the Ru crystal. Such a sample is shown in Fig. 3b exhibiting with Λ = (174 ± 10) Å very good long-range order, too. The best growth method for order is to combine CVD and C loading and segregation of the surface layer. Graphene layers such as the ones shown in Fig. 3a exhibit in contrast to former findings [18] well established graphene bands, however, the samples always contain a small fraction of 0.1 - 0.2 ML second layer [19].

We now describe the effect of a periodic potential on the electronic band structure of graphene resulting from the moiré structure of g/Ir(111) - (9.32 x 9.32) [20, 21] and from its reinforcement by self-assembled Ir clusters grown on-top [22]. For the first system, mostly unperturbed Dirac cones at the K-points of the Brillouin zone, except for the opening of minigaps at the boundaries of the mini-Brillouin zone, have been reported [23]. Figure 4 shows STM images and ARPES intensities comparing both systems revealing that the cluster superlattice potential induces a strong group velocity anisotropy together with a signicant band gap opening [22]. We focus on the energy region close to the apex of the Dirac cone and since the linear dispersion of the π-band is modified close to the Bragg planes, we restrict our analysis to energies $E - E_F > -0.5$ eV. In the presence of the superlattice the group velocities in both directions are $\upsilon_{\Gamma K}$ = (4.90 ± 0.06) eV Å/ħ and $\upsilon_{p\Gamma K}$ = (2.90 ± 0.05) eV Å/ ħ, corresponding to an anisotropy of $\Delta\upsilon/\upsilon_{p\Gamma K}$ = (70 ± 5)%. This

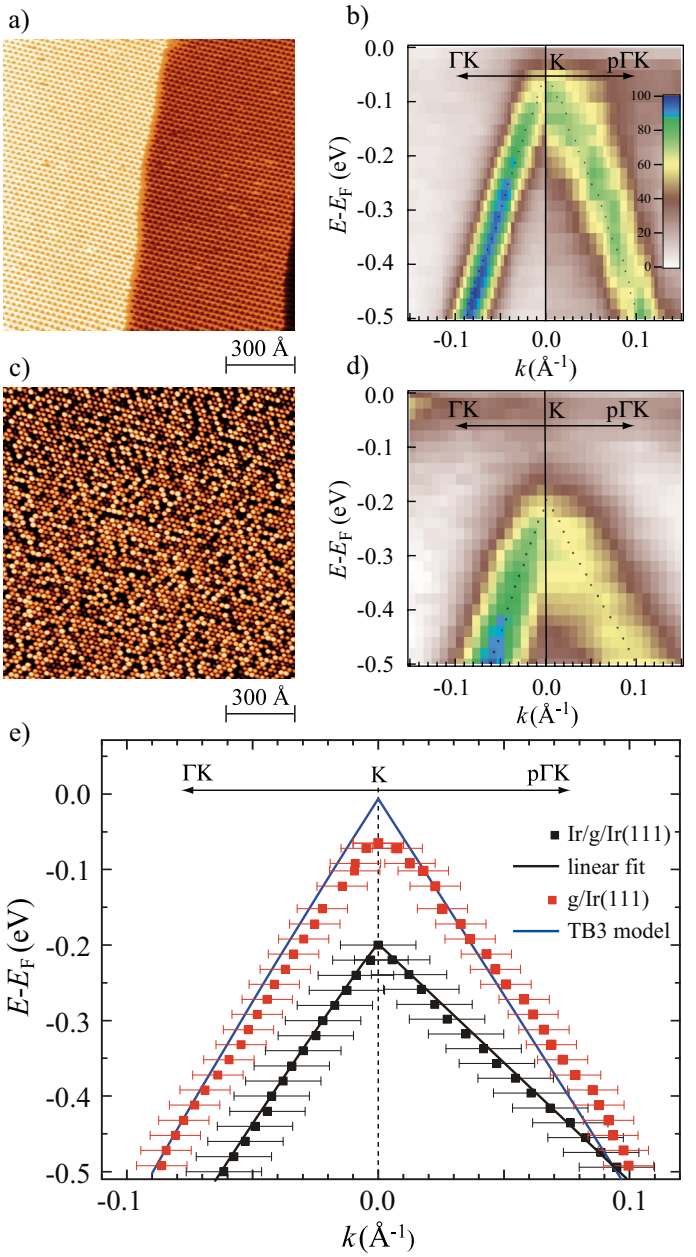

FIG. 4. a) STM image of the moiré structure of g/Ir(111) (T_{CVD} = 1300 K). b) ARPES intensity of the π-band of g/Ir(111) around the K-point and along the ΓK direction and perpendicular to it. c) STM image of Ir cluster superlattice grown on g/Ir(111) (Θ = 0.15 ML, T_{dep} = 375 K). d) ARPES intensity of the π-band of graphene for Ir/g/Ir(111). The dots represent the peak positions of the momentum distribution curves (MDCs). e) The valence band Dirac cone is clearly more asymmetric with the cluster superlattice (black) than without it (red). The error bars along k are the HWHM of the Lorentzian fits of the MDCs. Error bars in energy are with 20 meV comparatively small and therefore not shown.

value is 12 times larger than the anisotropy expected for unperturbed graphene due to the trigonal warping. A tight-binding approximation up to third-nearest neighbors (TB3 model) for free-standing graphene gives $\Delta v / v_{p\Gamma K}$ = 5% [24]. The anisotropy for g/Ir(111) is with $\Delta v / v_{p\Gamma K}$ = (16 ± 2)% larger than this, showing the small effect of the periodic potential resulting from the moiré alone. The group velocity renormalization is expected to be more effective for charge carriers moving perpendicularly to the largest corrugation of the potential [3, 4].

The superlattice induced band gap opening can be derived from comparing the positions of the Dirac cone summits for both cases, and by making reasonable assumptions on the position of the Dirac point derived from checking for charge neutrality. For g/Ir we find E_π = (-70 ± 20) meV in good agreement with previous results [25]. The Ir cluster superlattice shifts the π summit down to E_π = (-200 ± 20) meV, while the π*-band stays above E_F. Following literature [5, 25] we assume charge neutrality for g/Ir(111) and find $E_{g,\,g/Ir}$ = (140 ± 40) meV. For the cluster lattice E_D might be different due to charge transfer, which can be estimated from the core level and conduction band shifts. We find that the C1s level shifts down by (30 ± 30) meV and the top of the σ-band at the M point of the second Brillouin by the same amount. With E_D = -30 meV we find $E_{g,\,Ir/g/Ir}$ = 340 meV. For an interval of reasonable values of -35 meV ⩽ E_D ⩽ 50 meV for gr/Ir(111), we find that the cluster superlattice increases the bandgap by factors from 3.9 to 1.8. We are currently investigating the effect of alkali co-adsorption on the Ir superlattice which further increases the gap between the Dirac cones, however, it also shifts the bottom of the π*-band down below E_F.

Well defined graphene layers on single crystal metal surfaces have novel electronic properties strongly depending on their long-range order. Surface science techniques may be used to connect structure with property in order to derive a more profound understanding of how this new material interacts with metal contacts. In particular their strain distribution is expected to strongly influence the electronic structure. Eventually, graphene layers may also be used as a spacer layer separating magnetic nanostructures or impurities from magnetic or nonmagnetic substrates.

[1] Y. M. Lin *et al.*, Science, **327**, 662 (2010).
[2] A. L. Vazquez de Parga *et al.*, Phys. Rev. Lett., **100**, 056807 (2008).
[3] C. H. Park *et al.*, Phys. Rev. Lett., **103**, 046808 (2009).
[4] L. Brey and H. A. Fertig, Phys. Rev. Lett., **103**, 046809 (2009).
[5] P. J. Feibelman, Phys. Rev. B, **77**, 165419 (2008).
[6] K. S. Novoselov *et al.*, Science, **306**, 666 (2004).
[7] J. Hrbek, J. Vac Sci. Technol., A, **4**, 86 (1986).
[8] T. A. Land *et al.*, Appl. Phys. A, **53**, 414 (1991).
[9] T. Livneh and M. Asscher, J. Phys. Chem. B, **104**, 3355 (2000).
[10] W. J. Arnoult and R. B. McLellan, Scr. Metall., **6**, 1013 (1972).
[11] N. Weiss, Ph.D. thesis, EPFL (2004).
[12] P. W. Sutter, J.-I. Flege, and E. A. Sutter, Nat. Mater., **7**, 406 (2008).
[13] E. Loginova *et al.*, New J. Phys., **10**, 093026 (2008).
[14] D. Martoccia *et al.*, Phys. Rev. Lett., **101**, 126102 (2008).
[15] D. Martoccia *et al.*, N. J. Phys., **12**, 043028 (2010).
[16] W. Moritz *et al.*, Phys. Rev. Lett., **104**, 136102 (2010).
[17] The spatial 2D autocorrelation is defined as $ac_{i,j} = \sum_{k,l=1}^{n} z_{k,l} \cdot z_{k+i,l+j}$, i.e., the pixels of the image are multiplied with the ones of the same image translated by i, k.
[18] E. Sutter *et al.*, Appl. Phys. Lett., **94**, 133101 (2009).
[19] M. Papagno *et al.*, in preparation (2011).
[20] A. T. N'Diaye *et al.*, Phys. Rev. Lett., **97**, 215501 (2006).
[21] J. Coraux *et al.*, Nano Lett., **8**, 565 (2008).
[22] S. Rusponi *et al.*, Phys. Rev. Lett., **105**, 246803 (2010).
[23] I. Pletikosic *et al.*, Phys. Rev. Lett., **102**, 056808 (2009).
[24] S. Reich *et al.*, Phys. Rev. B, **66**, 035412 (2002).
[25] R. Balog *et al.*, Nat. Mater., **9**, 315 (2010).